

Effects of Coating and Stirring on Superparamagnetic Iron Oxide Nanoparticles Size and Magnetic Characteristics

Lida Ghazanfari¹, Mohammad E. Khosroshahi^{1,2}

Laser & Nanobiophotonic Lab., Biomaterials Group, Faculty of Biomed. Eng., Amirkabir University of Tech., Tehran, Iran¹

Advanced Diffusion-Wave Technologies (CADIFT), Department of Mechanical Eng. & Industry, University of Toronto, Canada²

ABSTRACT: Considering the importance of nanoparticles physico-chemical properties in biomedical applications, we intend to describe and compare the results of five experimental studies including: uncoated magnetic nanoparticles (MNPs), MNP + polyvinyl alcohol (PVA), MNP + amorphous silica (SiO₂) + gold (Au), and MNP + Au only. Controlled co-precipitation technique under N₂ gas is used to prevent undesirable critical oxidation of Fe²⁺. For uncoated Fe₃O₄ NPs with saturation magnetization (M_s) range of (40-100) emu/g, smaller particles are synthesized by decreasing the NaOH concentration and increasing the stirring speed with the smallest value corresponding to 7.5 nm using 0.9 M of NaOH at 1500 rpm. The coating process is done in four separate steps as follows: (i) the stable magnetic fluid containing well-dispersed Fe₃O₄/PVA nanocomposites which indicates a fast magnetic response with the smallest value of 7.5 nm using 0.9 M of NaOH at 750 rpm and M_s of 50 emu/g, (ii) the synthesized Fe₃O₄ NPs are stabilized using trisodium citrate (TSC) coating and then covered by SiO₂ layer using Stober method with the smallest value of 50 nm using 0.9 M of NaOH at 750 rpm and M_s of 30 emu/g, (iii) small gold colloids (1-3 nm) are synthesized using Duff method and covered the amino functionalized particle surface of Fe₃O₄/SiO₂ nanoshells with the smallest value of 85 nm using 0.9 M of NaOH at 750 rpm and M_s of 1.3 emu/g, (iv) also, bare superparamagnetic iron oxide NPs (SPIONs) are covered by a thin layer of gold alone with the smallest value of 16 nm using 0.9 M of NaOH at 1500 rpm and M_s of 12 emu/g. Magnetic properties and size of nanoshells are assessed using vibrating sample magnetometer (VSM) and transmission electron microscope (TEM). Furthermore, M_s of 7.5 nm magnetite is high enough to be used as contrast agent for photoacoustic (PAI) and magnetic resonance imaging (MRI).

KEYWORDS: SPION, Stirring rate, Coating materials, Magnetic characteristics, Biomedical applications.

I. INTRODUCTION

Magnetic field-responsive nanoparticles are specific subsets of smart materials that obey Coulomb's law, and can be manipulated by an external magnetic field gradient. In recent decades, magnetic nanoparticles (MNPs), especially maghemite (γ -Fe₂O₃) and magnetite (Fe₃O₄), have attracted increasing interest because of their outstanding properties including low toxicity [1]. Particle size, uniformity in size, chemical stability, and good magnetic response and biocompatibility are the main characteristics of the MNPs. Based on the mesoscopic physical and rheological properties of superparamagnetic iron oxide nanoparticles (SPION) [2], they offer a variety of applications in different areas such as colour imaging and magnetic recording [3], biotechnology and biomedicine, such as enzyme-immobilization [4], biosensing and bioelectrocatalysis [5], separation and purification [6], magnetic resonance imaging [7], protein [8] and drug delivery [9], and guided tumor therapy [10]. MNPs have sizes that place them at dimensions comparable to those of a virus (20-500 nm), a protein (5-50 nm), or a gene (2 nm wide and 10-100 nm long). Synthesis and characterization

International Journal of Innovative Research in Science, Engineering and Technology

(An ISO 3297: 2007 Certified Organization)

Vol. 4, Issue 7, July 2015

of high-quality iron oxide NPs have been investigated in the literature [11-14]. There are two methods of preparing Fe_3O_4 NPs: i- physical methods such as plasma [15], laser pyrolysis [16], electron beam lithography [17], gas phase deposition [9], and, ii- chemical method mainly using co-precipitation technique [18]. The difficulty in the synthesis of ultrafine particles arises from the high surface energy of these systems. The MNPs can be coated with a biocompatible and diamagnetic material to prevent the formation of large aggregates of MNPs and to functionalize for biological agents attachment [19]. For example, coating of SPIONs with polyvinyl alcohol (PVA) prevents their aggregation via steric hindrance mechanism and leads to the formation of monodispersed nanocrystals [20]. Similarly, encapsulating the SPIONs in silica yields a unique magnetic responsivity as well as making them suitable for biomedical applications [21,22]. The SPIONs are coated with silica via the sol-gel process [23,24]. The outer surface of silica layer can be easily modified with amine groups by formation of covalent bonds [25]. These free amine groups would facilitate the initial growth and the resultant growth of the nanogold. Gold nanoshells can be an attractive agents for both diagnostic and therapeutic applications [26,27]. Kim and co-workers studied a new design of magneto-plasmonic nanostructures for both MRI and photothermal therapy [28]. In this paper, it is intended to describe the results of SPIONs synthesis using different coatings and magnetic stirring and consequently their effects on the magnetic properties which can influence the biomedical applications.

II. PROPOSED METHODOLOGY

Chemicals and reagents:

All analytical reagents are used without further purification. Ferric chloride hexahydrate ($\text{FeCl}_3 \cdot 6\text{H}_2\text{O}$, 99%), ferrous chloride tetrahydrate ($\text{FeCl}_2 \cdot 4\text{H}_2\text{O}$, 99%), (HCl, 37%), sodium hydroxide (NaOH, 99%), absolute ethanol, polyvinyl alcohol (PVA) of 30000-40000 g mol^{-1} nominal molecular weight and 86-89% degree of hydrolysis, trisodium citrate (TSC), ammonia aqueous (25 wt%), $\text{Si}(\text{OC}_2\text{H}_5)_4$ (tetraethyl orthosilicate, TEOS) are purchased from Merck. 3-aminopropyltriethoxysilane (APTS), tetrakis(hydroxymethyl) phosphonium chloride (THPC), gold (iii) chloride trihydrate ($\text{HAuCl}_4 \cdot 3\text{H}_2\text{O}$, $\geq 49\%$ Au basis), potassium carbonate (K_2CO_3), and formaldehyde solution (H_2CO , 37%) are obtained from Sigma-Aldrich (St. Louis, MO). Deionized water (specific conductance 0.1 $\mu\text{S/cm}$) is provided by a milli-Q system and deoxygenated by bubbling N_2 gas for 1 hour prior to use. All the main synthesizing steps are carried out by passing N_2 gas through the solution media.

Synthesis of Fe_3O_4 NPs:

Stock solutions of 1.28 M of $\text{FeCl}_3 \cdot 6\text{H}_2\text{O}$, 0.64 M of $\text{FeCl}_2 \cdot 4\text{H}_2\text{O}$ and 0.4 M of HCl are dissolved in deionized water as the iron source. 25 ml of iron source is added into 250 ml of alkali source of (0.9-1.5) M of NaOH under vigorous stirring for 30 min at room temperature under N_2 gas. The synthesized Fe_3O_4 samples are classified as S1-S4, S¹1-S⁴4, and S¹¹1-S⁴⁴4 using 0.9, 1.1, 1.3 and 1.5 M of NaOH concentration under magnetic stirring conditions of 450, 750, and 1500 rpm, respectively. By maintaining a molar ratio of $\text{Fe}^{2+} : \text{Fe}^{3+} = 1:2$ between pH of 7.5-14, Fe_3O_4 should be completely precipitated. The powder is washed and centrifuged twice. Then 0.01M of HCl is added to neutralize the anionic charge on the particle surface. The cationic colloidal particles are separated by centrifugation and peptized by watering.

PVA coated Fe_3O_4 NPs fabrication:

Fe_3O_4 NPs are coated with PVA shell to prevent them from possible oxidation and agglomeration. 4 gr of PVA is dissolved in water and added to the Fe_3O_4 solution, then it is heated at 90 °C for 30 min under appropriate magnetic stirring (750 rpm). The samples are classified as S5-S8 where the samples are synthesized using 0.9, 1.1, 1.3 and 1.5 M of NaOH concentration corresponds to S5, S6, S7 and S8, respectively. The obtained magnetic product is collected by magnetic separation. After that, the solution is washed, centrifuged and peptized for three times, then freeze-dried.

Coating of citrate-modified Fe_3O_4 with silica:

The uncoated Fe_3O_4 mud is redispersed in 200 ml of trisodium citrate solution (0.5 M) and heated at 90 °C for 30 min under magnetic stirring (750 rpm). In order to remove the excessive citrate groups adsorbed on the Fe_3O_4 NPs, they are precipitated with acetone and collected with a magnet and then washed. The solution is centrifuged and peptized twice, then freeze-dried. The coating of citrate-modified Fe_3O_4 (only sample S1 as an optimized one) with silica is carried out based on the Stober method, with some modifications. The obtained powder is suspended in water, sonicated and then

is adjusted to 2 wt%. 2 g of this powder is first diluted with water (40 ml), ethanol (120 ml), and then concentrated aqueous ammonia (3 ml) is added [24] and sonicated. 0.9 g of TEOS diluted in ethanol (20 ml) is added to this

International Journal of Innovative Research in Science, Engineering and Technology

(An ISO 3297: 2007 Certified Organization)

Vol. 4, Issue 7, July 2015

dispersion under mechanical stirring. After 12 h, the solution is washed, centrifuged and peptized for three times.

Coating Fe₃O₄/SiO₂nanocomposites with gold:

65 µl of APTS is added to a 200 ml of the Fe₃O₄/SiO₂ nanoshellsolution according to the approximate concentration and surface area of the silica layer. The mixture is vigorously stirred and refluxed for 1 hour. Then NaOH of 1 M (0.5 ml) and THPC solution (1 ml) is added to a 45 ml of deionized water and the mixture is stirred for 5 minutes. Then, the solution is added to 2 ml of 1% HAuCl₄ to obtain gold colloids which are 2-3 nm in size. After that 5 ml of gold colloid solution is added to 1 ml of APTS-functionalized silica NPs dispersed in ethanol. The mixture is stored at 4 °C overnight to maximize the attachment of THPC gold nanoseeds onto the silica surface. A plating solution is prepared by mixing 3 ml HAuCl₄ (1%) with 200 ml of K₂CO₃ (1.8 mM) and aged for 48 hours. 4 ml of plating solution is then added to 200 µl of the solution containing the Fe₃O₄/SiO₂/Au nanocomposites[29]. By reduction of gold solution with H₂CO in the presence of Fe₃O₄/SiO₂/Au nanocomposites, the gold nanoshells are prepared.

Au nanoshell fabrication:

Uncoated Fe₃O₄ NPs (0.074 g), synthesized under magnetic stirring of 1500 rpm, are dispersed in 25 ml of ethanol by sonication. This suspension is diluted to 150 ml by 1 ml of deionized water and ethanol. 35 µl of APTS is added to the prepared suspension under vigorous magnetic stirring for 7 hours at room temperature. After that, amino-functionalized Fe₃O₄ NPs are washed for 5 times and then freeze-dried. Gold nanoshell precursor particles are prepared by adding 1 ml of amine-functionalized Fe₃O₄ NPs into 40 ml of THPC gold solution and 4 ml of 1 M NaCl and left for 12 hours at 4°C. Gold nanoshell is fabricated by adding 1 ml of precursor suspension to 9 ml of plating solution. 50 µl of H₂CO is added into a 10 ml prepared suspension of precursor NPs in plating solution and aged for 15 min as suggested [30]. The obtained Fe₃O₄/Aunanoshells are washed and collected by centrifuge.

Characterization:

Transmission electron microscopy (TEM) is performed using a Phillips CM-200-FEG microscope operating at 120 kV. Magnetization measurements are carried at 300 K in a magnetic field (H) of up to 20 kOe with a vibrating sample magnetometer (MeghnatisDaghighKavir Co. VSM/AGFM) that can measure magnetic moments as low as 10⁻³ emu. For the magnetization measurements, uncoated Fe₃O₄ NPs are in dry powder form obtained by evaporating the water from the solution. Sonication is done using steel probe sonicator (output: 400 W, model: Branson 450, Digital Sonifer®, Danbury, CT). The samples are dried by freeze dryer (Pishtaz Engineering Co. Model: FD-4).

III. EXPERIMENTAL RESULTS AND DISCUSSION

TEM:

The bright field TEM micrographs are used to observe the agglomeration state, particle size distribution, and morphology of particles at different steps of nanostructure fabrication.

(a) Synthesis under magnetic stirring of 750 rpm:

Fig. 1 shows the variation of particle size with NaOH concentration. As it is seen in this figure, particle size decreases at lower NaOH %, which in our case this corresponds to 35 nm at 0.9 M of NaOH. As shown in Fig. 1b,c, the synthesized Fe₃O₄ powder consists of almost dispersed particles. Due to large specific surface area, high surface energy, and magnetostatic force which favors the formation of magnetically aligned chains of magnetic dipoles, some of the primary NPs are aggregated into secondary particles.

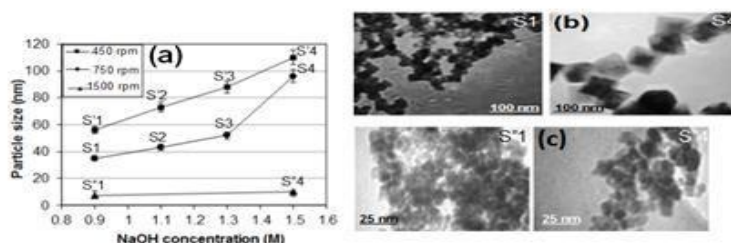


Figure 1: (a) Particle size vs NaOH concentration for uncoated Fe₃O₄ NPs at various rpm, TEM micrographs of uncoated Fe₃O₄ NPs: (b) (S1, S4) and (c) (S¹, S⁴).

International Journal of Innovative Research in Science, Engineering and Technology

(An ISO 3297: 2007 Certified Organization)

Vol. 4, Issue 7, July 2015

The mean particle size of PVA-coated Fe₃O₄ NPs is examined by TEM imaging (Fig. 2).

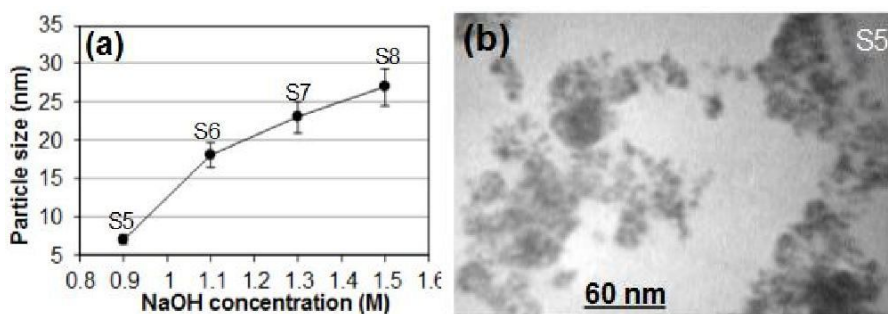


Figure 2: (a) Particle size vs NaOH concentration for PVA coated Fe₃O₄ NPs (S5-S8) at 750 rpm, (b) TEM of PVA-coated Fe₃O₄ NPs (S5)

In ferrofluid, stability is maintained by electrostatic and repulsive interactions between counterions and amphoteric hydroxyl ions. SiO₂ coating is formed under polycondensation process. Due to TEOS hydrolysis, -OCH₂CH₃ is transferred into -OH. As shown in figure 3, SiO₂ coated Fe₃O₄ NPs have a mean diameter of 50 nm and have a rough surface, which is comparable with the results obtained by Deng et al. [21].

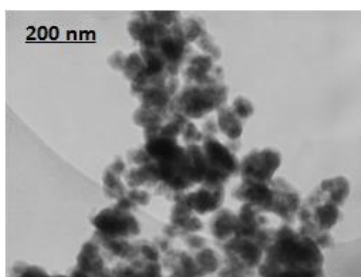


Figure 3: TEM of Fe₃O₄/SiO₂ nanoshells at 750 rpm at 0.9 M of NaOH

The gold layer can stabilize the magnetic particles by sheltering the magnetic dipole interaction. Amine-functionalized NPs exhibited heavy clusters of small gold NPs assembled on the surfaces of silica as shown in Fig. 4 which is comparable to that reported by Serhsen et al. [31].

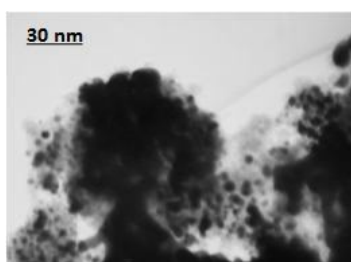


Figure 4: TEM of Fe₃O₄/SiO₂/Au nanostructures at 750 rpm at 0.9 M of NaOH

International Journal of Innovative Research in Science, Engineering and Technology

(An ISO 3297: 2007 Certified Organization)

Vol. 4, Issue 7, July 2015

(b) At 1500 rpm:

As seen in Fig. 5, the effective mean diameter of gold coated Fe₃O₄ NP is 16 nm.

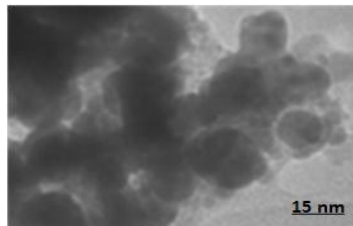


Figure 5: TEM of Fe₃O₄/Au nanoshells at 1500 rpm at 1.5 M of NaOH

VSM

Considering the magnetism of a magnetic material, saturation magnetization, (M_s) and coercivity, (H_c) are among the main magnetic parameters that have to be evaluated. Magnetization measurements are carried at 300 K in a magnetic field (H) of up to 20 kOe with a vibrating sample magnetometer (MeghnatisDaghighKavir Co. VSM/AGFM-Iran) that can measure magnetic moments as low as 10^{-3} emu.

(a) At 750 rpm:

The value of M_s for these particles is measured about 82 emu/g (Fig. 6) which is close to the bulk value of magnetite (85-100 emu/g) [32]. In our case, the M_s value for S1 is slightly higher than that reported by Yang et al. [23]. The saturation magnetization of Fe₃O₄ NPs increases with increase in particle size, as reported in the literature [33]. Moreover, this increase in M_s may be the result of different chemical composition on the surface like oxidation of magnetite to maghemite and surface effect such as nonlinearity of spins of magnetically inactive layer with the magnetic field [34].

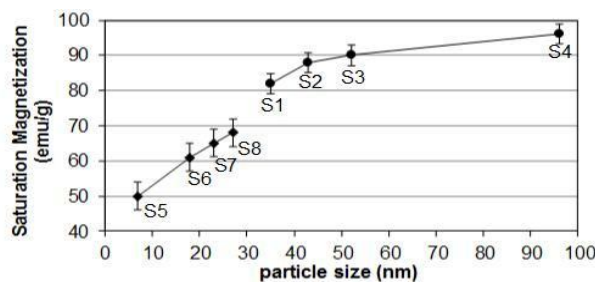


Figure 6: Variation of saturation magnetization with particle size for bare Fe₃O₄ NPs (S1-S4) and PVA-coated Fe₃O₄ NPs (S5-S8) at 750 rpm

The corresponding values of H_c were measured as 119 and 82 Oe for particles sizes of 35 nm and 96 nm, respectively, see Figure 7.

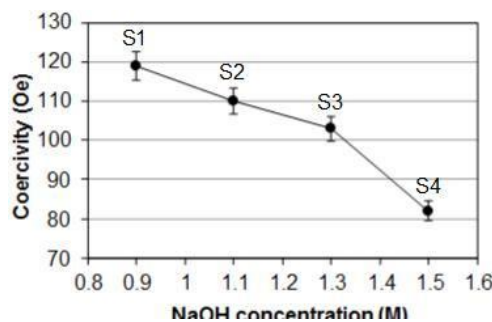


Figure 7: Variation of coercivity with particle size for bare Fe₃O₄ NPs at 750 rpm

International Journal of Innovative Research in Science, Engineering and Technology

(An ISO 3297: 2007 Certified Organization)

Vol. 4, Issue 7, July 2015

These results suggest that H_c is strongly size dependent. Due to domain wall motion, the bulk samples with sizes larger than the domain wall width can cause magnetization reversal. Domain walls can become pinned at grain boundaries as they move through a sample and additional energy would be needed to keep moving. Grain size dependence of coercivity and permeability (GSDCP) theory predicts:

$$H_c = P_1 \frac{\sqrt{AK}}{D_g} \quad (1)$$

where A denotes the exchange constant, K is a magneto crystalline anisotropy constant, P_1 and P_2 are dimensionless factors. Subsequently, reducing the grain size, D_g , increases H_c by creating more pinning sites. For ultrafine particles, the modified form of theory predicts:

$$H_c = P_2 \frac{K^4 D_g^6}{M_s A} \quad (2)$$

The difference between equations (1) and (2) is defined by ferromagnetic exchange length as:

$$L_{ex} = \sqrt{\frac{A}{K}} \quad (3)$$

Using the following parameters for magnetite ($K=1.35 \times 10^4 \text{ J/m}^3$, $A=10^{-11} \text{ J/m}$), the exchange length can be estimated as $L_{ex}=27 \text{ nm}$. Fig. 6 shows the magnetization values of PVA coated Fe_3O_4 NPs obtained by VSM at room temperature. The M_s value for these particles is measured about 50 emu/g which steadily increased with increase in their size.

The magnetization curve of $\text{Fe}_3\text{O}_4/\text{SiO}_2$ nanoshells show no remanence i.e. the curve passes through the origin. When the TEOS is added, the M_s value of the resultant $\text{Fe}_3\text{O}_4/\text{SiO}_2$ nanoshells decreased to 30 emu/g. Insignificant coercivity and remanence with no hysteresis loop is observed for magnetite-silica NPs which likely implies their superparamagnetic behaviour. Similarly, the magnetization curve of the $\text{Fe}_3\text{O}_4/\text{SiO}_2/\text{Au}$ nanocomposites exhibit M_s value of 1.3 emu/g with no remanence and coercivity.

(b) At 1500 rpm:

The M_s value of uncoated Fe_3O_4 NPs is determined to be 48 emu/g at 1.5 M of NaOH (Fig. 8) which decreased to the 12 emu/g for gold nanoshells. In our case, the M_s value of the nanoshells is larger than that reported by Z. Xu et al. [35]. Melancon et al. elucidated that their synthesized gold coated magnetic-silica NPs with the M_s of 0.4 emu/g can be used as contrast agent in MRI [36]. Therefore, all of our fabricated nanostructures can be considered as good candidates for MRI application.

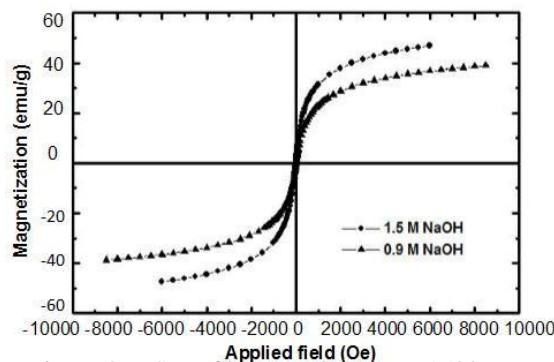


Figure 8: VSM of bare Fe_3O_4 NPs at 1500 rpm

IV. CONCLUSION

In this research, we intend to synthesize, characterize and compare the results of uncoated with polymer, ceramic, and metal coated Fe_3O_4 NPs. The controlled co-precipitation technique is used to prepare superparamagnetic iron oxide NPs with least diameter value of 7.5 nm using 0.9 M NaOH. The particle size of magnetite colloidal nanocrystals are influenced by changes in the base molarity. It is also, shown that by optimizing the preparation condition using PVA, silica, and gold as coating materials, a stable magnetic fluid containing well-defined core-shell structures can be achieved. A systematic study of the formation and characterization of different core-shell nanostructures is performed.

International Journal of Innovative Research in Science, Engineering and Technology

(An ISO 3297: 2007 Certified Organization)

Vol. 4, Issue 7, July 2015

These results provided a conceptual understanding of the structural and magnetic properties for these binary and tertiary NPs. The high saturation magnetization of nanostructures makes them suitable for MRI applications. Additionally, NPs with suitable both optothermal and magnetic properties are also frequently used in photo-acoustic imaging of tissues as contrast agent. Furthermore, uniform dispersion would make all the synthesized nanostructures potential candidates for biomedical applications.

REFERENCES

- [1] X. Qiao, J. Zhou, B.P. Binks, X. Gong, K. Sun, "Magnetorheological behavior of Pickering emulsions stabilized by surface modified Fe_3O_4 nanoparticles", *Colloids and Surfaces A: Physicochem. Eng. Aspects*, vol. 412, pp. 20–28, 2012.
- [2] M. E. Khosroshahi, L. Ghazanfari, "Comparison of magnetic and rheological behavior of uncoated and PVA coated Fe_3O_4 nanoparticles synthesized under N_2 gas", *J. Magn. Magn.Mater.*, vol. 324, pp. 4143-4146, 2012.
- [3] J. Popplewell, L. Sakhini, "The dependence of the physical and magnetic properties of magnetic fluids on particle size", *J. Magn.Magn.Mater.*, vol. 149, pp. 72-78, 1995.
- [4] J. R. McCarthy, Ralph Weissleder, "Multifunctional magnetic nanoparticles for targeted imaging and therapy", *Adv. Drug Delivery Reviews*, vol. 60, pp. 1241–1251, 2008.
- [5] R. De Palma, C.X. Liu, F. Barbagini, G. Reekmans, et al, "Magnetic particles as labels in bioassays: interactions between a biotinylated gold substrate and streptavidin magnetic particles", *J. Phys. Chem. C*, vol.111, pp.12227–12235, 2007.
- [6] X.Q. Xu, C.H. Deng, M.X. Gao, W.J. Yu, et al, "Synthesis of magnetic microspheres with immobilized metal ions for enrichment and direct determination of phosphopeptides by matrix-assisted laser desorption ionization mass spectrometry". *Adv. Mater.* 18 () 3289-3293, 2006.
- [7] C. Corot, Ph. Robert, J. Idée, M. Port, "Recent advances in iron oxide nanocrystal technology for medical imaging", *Adv. Drug Delivery Reviews*, vol. 58, pp. 1471-1504, 2006.
- [8] L. Xu, M.J. Kim, K.D. Kim, Y.H. Choa, H.T. Kim, "Surface modified Fe_3O_4 nanoparticles as a protein delivery vehicle", *Colloids and Surfaces A: Physicochem. Eng. Aspects*, vol. 350, pp. 8–12, 2009.
- [9] B. Chertok, A.E. David, B.A. Moffat, V.C. Yang, "Substantiating in vivo magnetic brain tumor targeting of cationic iron oxide nanocarriers via adsorptive surface masking", *Biomaterials*, vol. 30, pp. 6780-6787, 2009.
- [10] S. Kayal, R.V. Ramanujan, "Doxorubicin loaded PVA coated iron oxide nanoparticles for targeted drug delivery", *Mater.Sci. Eng. C*, vol. 30, pp. 484-490, 2010.
- [11] M. E. Khosroshahi, L. Ghazanfari and M. Tahriri, "Characterization of binary ($\text{Fe}_3\text{O}_4/\text{SiO}_2$) biocompatible nanocomposites as magnetic fluid", *J. of Exp.Nanosci.*, vol. 6, pp. 1–16, 2011.
- [12] M. E. Khosroshahi, L. Ghazanfari, "Amino surface modification of $\text{Fe}_3\text{O}_4/\text{SiO}_2$ nanoparticles for bioengineering applications", *Surf. Eng.*, vol. 27, pp. 573-580, 2011.
- [13] M. E. Khosroshahi, L. Ghazanfari, "Synthesis and functionalization of SiO_2 coated Fe_3O_4 nanoparticles with amino groups", *Mat. Sci. Eng. C*, vol. 32, pp. 1043–1049, 2012.
- [14] M. Tajabadi, M. E. Khosroshahi, S. Bonakdar, "An efficient method of SPION synthesis coated with third generation PAMAM dendrimer", *Colloids and Surfaces A: Physicochem. Eng. Aspects*, vol. 43, pp. 18– 26, 2013.
- [15] F.G. Mondalek, Y.Y. Zhang, B. Kropp, R.D. Kopke, et al, "The permeability of SPION over an artificial three-layer membrane is enhanced by external magnetic field", *J. Nanobiotech.*, vol. 4, pp. 1-9, 2006.
- [16] N. Gribanov, E. Bibik, O. Buzunov, V. Naumov, "Physico-chemical regularities of obtaining highly dispersed magnetite by the method of chemical condensation", *J. Magn. Magn.Mater.*, vol. 85, pp. 7-10, 1990.
- [17] K. Kamei, Y. Mukai, H. Kojima, T. Yoshikawa, M. Yoshikawa, et al, "Direct cell-entry of gold/iron-oxide magnetic nanoparticles in adenovirus mediated gene delivery", *Biomaterials*, vol. 30, pp. 1809-1814, 2009.
- [18] A. Gupta, S. Wells, "Surface-modified superparamagnetic nanoparticles for drug delivery: preparation, characterization, and cytotoxicity studies", *IEEE Trans Nanobioscience*, vol. 3, pp. 66–73, 2004.
- [19] J. E. Rosen, L. Chan, D. B. Shieh, F. Gu, "Surface functionalization of superparamagnetic iron oxide nanoparticles for cancer diagnosis and targeted therapy", *Nanomed: Nanotech., Biology and Medicine*, vol. 8, pp. 275-290, 2012.
- [20] M. Sairam, B.V.K. Naidu, S.K. Nataraj, B. Sreedhar, T.M. Aminabhavi, "Poly(vinyl alcohol)-iron oxide nanocomposite membranes for pervaporation dehydration of isopropanol, 1,4-dioxane and tetrahydrofuran", *J. Membr. Sci.*, vol. 283, pp. 65–73, 2006.
- [21] Y.H. Deng, C.C. Wang, J.H. Hu, W.L. Yang, Sh.K. Fu, "Investigation of formation of silica-coated magnetite nanoparticles via sol-gel approach", *Colloids and Surfaces A: Physicochem. Eng. Aspects*, vol. 262, pp. 87-93, 2005.
- [22] R. Alwai, S. Telenkov, A. Mandelis, T. Leshuk, F. Gu, K. Michaelian, "Silica-coated super paramagnetic iron oxide nanoparticles (SPION) as biocompatible contrast agent in biomedical photoacoustics", *Biomed. Opt. Express*, vol. 1, pp. 2500-9, 2012.
- [23] Z. Lu, J. Dai, X. Song, G. Wang, W. Yang, "Facile synthesis of $\text{Fe}_3\text{O}_4/\text{SiO}_2$ composite nanoparticles from primary silica particles", *Colloids and Surfaces A: Physicochem. Eng. Aspects*, vol. 317, pp. 450–456, 2008.
- [24] D. Yang, J. Hu, S. Fu, "Controlled synthesis of magnetite-silica nanocomposites via a seeded sol-gel approach", *J. Phys. Chem. C*, vol. 113, pp. 7646-7651, 2009.
- [25] E. A. Smith, W. Chen, "How to prevent the loss of surface functionality derived from aminosilanes", *Langmuir*, vol. 24, pp. 12405-9, 2008.
- [26] M. E. Khosroshahi, M. Nourbakhsh, "In vitro skin wound soldering using SiO_2/Au nanoshells and a diode laser", *Med. Laser Appl.*, vol. 26, pp. 35-42, 2011.
- [27] L. Ghazanfari, M. E. Khosroshahi, "Simulation and experimental results of optical and thermal modeling of gold nanoshells", *Materials Science and Engineering C*, vol. 42, pp.185–191, 2014.
- [28] J. Kim, S. Park, J.E. Lee, S.M. Jin, J.H. Lee, et al, "Designed fabrication of multifunctional magnetic gold nanoshells and their application to magnetic resonance imaging and photothermal therapy", *Angew. Chem. Int Ed.*, vol. 45, pp. 7754-7758, 2006.
- [29] M. E. Khosroshahi, L. Ghazanfari, "Physicochemical characterization of $\text{Fe}_3\text{O}_4/\text{SiO}_2/\text{Au}$ multilayer nanostructure", *Mater. Chem. Phys.*, vol.

International Journal of Innovative Research in Science, Engineering and Technology

(An ISO 3297: 2007 Certified Organization)

Vol. 4, Issue 7, July 2015

133, pp. 55– 62, 2012.

[30] Z. Hassannejad, M. E. Khosroshahi, "Synthesis and evaluation of time dependent optical properties of plasmonic–magnetic nanoparticles", *Optical Materials*, vol. 35, pp. 644-651, 2013.

[31] S.R. Sershen, S.L. Westcott, S.J. Oldenburg, T.R. Lee, N.J. Halas, "Formation and adsorption of clusters of gold nanoparticles onto functionalized silica nanoparticle surfaces", *Langmuir*, vol. 14, pp. 5396-5401, 1998.

[32] W. Yu, T. Zhang, J. Zhang, X. Qiao, L. Yang, Y. Liu, "The synthesis of octahedral nanoparticles of magnetite", *Mater. Lett.*, vol. 60, pp. 2998-3001, 2006.

[33] S. Mohapatra, N. Pramanik, S. Mukherjee, S. K. Ghosh, P. Pramanik, "A simple synthesis of amine-derivatized superparamagnetic iron oxide nanoparticles for bioapplications", *J. Mater. Sci.*, vol. 42, pp. 7566-7574, 2007.

[34] R.D. Ambastha, P.K. Wattal, S. Singh, D. Bahadur, "Nano-aggregates of hexacyanoferrate loaded magnetite for removal of cesium from radioactive wastes", *J. Magn. Mater.*, vol. 267, pp. 335-340, 2003.

[35] Z. Xu, Y. Hou, S. Sun, "Magnetic core/shell $\text{Fe}_3\text{O}_4/\text{Au}$ and $\text{Fe}_3\text{O}_4/\text{Au}/\text{Ag}$ nanoparticles with tunable plasmonic properties", *J. Am. Chem. Soc.*, vol. 129, pp. 8698-9, 2007.

[36] M.P. Melancon, W. Lu, M. Zhong, M. Zhou, G. Liang, et al, "Targeted multifunctional gold-based nanoshells for magnetic resonance-guided laser ablation of head and neck cancer", *Biomaterials*, vol. 32, pp. 7600-8, 2011.